University of Tehran Press

Online ISSN: 2345-475X

DESERT

Home page: https://jdesert.ut.ac.ir/

# Assessing the aridity indices in Northeast Iran: implications for climate change and agricultural water management

**Zahra Shirmohammadi Aliakbarkhani[1*], Farid Foroughi[2*], Sayed farhad Saberali[3], Hossien Nastari Nasrabadi[1], Mohammad Naser Modoodi[1]**

[1] Faculty of Agriculture and Animal Science, University of Torbat-e Jam, Torbat-e Jam, Khorasan Razavi, Iran.
E-mail: shirmohammadi@tjamcaas.ac.ir

[2] College of Agriculture and Natural Resources of Darab, Shiraz University, Darab, Fars, Iran.
Email: foroughi@shirazu.ac.ir

[3] Department of Agronomy, Faculty of Agriculture, University of Tarbiat Modares, Tehran, Iran.

## Article Info.

**Article type:**
Research Article

**Article history:**
Received: 17 Jan. 2024
Received in revised from: 11 Mar. 2024
Accepted: 07 May 2024
Published online: 27 June 2024

**Keywords:**
Agricultural water resources,
Drought events,
Reference evapotranspiration,
Spatial-temporal variation,
Water security.

## ABSTRACT

Aridity indices have been widely applied in dividing climate regimes and monitoring drought events. The knowledge of the aridity index and reference evapotranspiration is very important not only for understanding climate change and its effects on ecosystem stability but also for managing agricultural water resources. Therefore, in this work, we studied the spatial-temporal variation and trend of ETo, $T_{mean}$, and four aridity indices, such as the De Martonne aridity index, Pinna combinative index, FAO aridity index, and Thornthwaite aridity index, and its climatic attribution in Northeast Iran using the observed climate records from 10 synoptic meteorological stations from 1950 to 2021. The results showed that ETo for Northeast Iran as a whole exhibited an increase at a rate of +9.65 $mmyr^{-1}$; $T_{mean}$ showed an increasing trend at the rate of 0.03 ºC $year^{-1}$ from the beginning of the statistical period of each station until 2021. Also, the $AI_T$, $AI_{DM}$, $AI_P$, and $AI_F$ increased significantly by +0.001, -0.03, -0.01, and -0.001 $year^{-1}$, respectively. Approximately 100% of stations showed an increasing trend in $AI_T$ and $AI_F$, while 50% of stations reached up to a significant increasing level, and about 60% of stations showed an increasing trend in $AI_{DM}$ and $AI_P$, while 70% of stations reached a significantly increasing level, which demonstrated that Northeast Iran was getting drier for the recent 40 years. This analysis of this study enhances the understanding of the relationship between climate change and drought in Northeast Iran, may be helpful for the agricultural irrigation system.

**Cite this article:** Shirmohammadi Aliakbarkhani, Z., Foroughi, F., Saberali, S.F., Nastari Nasrabadi, H., Naser Modoodi, M. (2024). Assessing the aridity indices in Northeast Iran: Implications for climate change and agricultural water management. DESERT, 29 (1), DOI: 10.22059/jdesert.2024.97810


DOI: 10.22059/jdesert.2024.97810

Publisher: University of Tehran Press

## 1. Introduction

Intensified human activities and global climate changes have led to significant impacts on ecohydrological patterns and quality and the quantity of water resources. The decreased water quantity resulted in the high frequency of drought events in arid or semi-arid regions (Zhuguo *et al*., 2004; Li *et al*., 2007; McVicar *et al*., 2007; Xu *et al*., 2007; X. Zhang *et al*., 2009; Q. Zhang *et al*., 2009a; Moral *et al*., 2016). During the last three decades, in any other decades after 1850, the climate has been warmer; in such circumstances, the water vapor capacity of the air increases, and it is expected to increase the amount of evapotranspiration (IPCC, 2013). This change has been identified not only in some climatic factors, such as rainfall, air temperature, and pan evapotranspiration but also its effects on all elements of water supply and hydrologic cycle such as precipitation, infiltration, groundwater, runoff, soil moisture, and reference evapotranspiration (ETo) in a variety of ways (Huntington, 2006; Zhang *et al*., 2011). These changes may be varied to a large region or may be limited to any one continent or a specific area (Kukal and Irmak, 2016). For example, Evapotranspiration has increased over the past few decades (Herath *et al*., 2018), but it has been decreasing in most parts of the world (Xu *et al*., 2007; Hosseinzadeh Talaee *et al*., 2014). Therefore, this climate change is expected to alter regional conditions. Among all atmospheric variables, evapotranspiration is a vital component of the global energy balance and the hydrological cycle contributing to environmental Equilibrium *(Wang et al*., 2007; Zhang *et al*., 2007). Furthermore, precipitation and evapotranspiration as excellent indicators for activity and analysis the water cycle and climate change are of great importance within the IPCC literature, determining surface runoff and groundwater recharge. In recent decades, extensive research efforts have examined the potential impact of climate change on aridity, ETo, and P and achieved beneficial results (Wang *et al*., 2014; Lang *et al*., 2017). Many recent studies have denoted that climate variation increases drought, aggravates the process of desertification, and changes precipitation patterns. This knowledge of aridity contribute to the understanding of drought disasters and increasing flood in many regions*(Goyal, 2004; Paltineanu et al., 2007; X. Zhang et al*., 2009; Zhang *et al*., 2009a,b). For this purpose, the aridity indices can be widely used to monitor droughts and climate-based land classification *(Hrnjak et al*., 2014; Moral *et al*., 2016; Gebremedhin *et al*., 2018). Aridity has been defined in a large range of indices, in the context of different fields such as hydrology, climatology and, which vary by the inclusion of several variables (Jain *et al*., 2010; Tatli and Türkeş, 2011; Vasiliades *et al*., 2011; Gao *et al*., 2015; Kukal and Irmak, 2016). Some kind of Aridity indices, such as De Martonne's aridity index(de Martonne, 1926), are often expressed as a function of precipitation and temperature. Also, Other aridity indices (AI) are a function of potential Evapotranspiration (ETo) and Precipitation, either as the long-term difference between potential Evapotranspiration (ETo) and Precipitation (P) giving the climatic water deficit, or as the ratio of Precipitation (P) and potential Evapotranspiration (ETo) have been considered good indicators of the severity of drought, can be used in the estimation of the impacts of climate change and climate classification scheme (Thornthwaite, 1948; Shifteh Some'e *et al*., 2013; Djaman *et al*., 2015). (Ullah *et al*., 2022) examined changes in five drought indices globally. Their findings indicated that the highest levels of aridity and its widespread expansion globally occurred predominantly in the recent decades (1991–2019),

particularly concentrating in equatorial and subtropical regions around the world.

Consequently, understanding of the spatiotemporal variations of potential Evapotranspiration (ETo) and knowledge of aridity have some value in evaluating and forecasting the agricultural water requirements and regional water resources, agricultural production, and irrigation planning (Arora, 2002; Paltineanu *et al*., 2007; Liang *et al*., 2010; Huo *et al*., 2013; Hrnjak *et al*., 2014; Moral *et al*., 2016). The Northeast Iran is located in an arid and semi-arid climate, that water shortage is one of the main problems in this area. As a result, this region experienced droughts with different magnitudes in different years. However, despite the importance of this issue, few studies have been carried out on the aridity in other regions of Iran (Tabari and Aghajanloo, 2013; Nouri and Bannayan, 2019), but no comprehensive research on the spatiotemporal aridity indices in this area have been published. Therefore, the present study focused on assessing the spatiotemporal distribution of aridity indices in Northeast Iran. The findings of this study will improve our understanding of climatic aridity, climate change, and the influence of aridity in the Northeast of Iran, and it provides useful information for agricultural water management.

## 2. Materials and methods

### *2.1. Study area and data description*

The Khorasan Razavi province is a geographical region located in the northeast part of Iran between latitude 33°-38° N and longitude of 56°-62° E. It has a total area of 117200 $km^2$, mean daily temperature varied from 12.8 to 19.4°C, with a seasonal average temperature ranging from 2.7 to 8.3°C in winter, from 17.9 to 25.2°C in spring, from 22.7 to 29.1°C in summer and from 7.6 to 12.8°C in autumn. Also, annual mean of precipitation varied from 129 to 317 mm, which primarily occurred in spring, winter, and autumn. Map of all districts of Khorasan Razavi province are shown in Figure 1.

The locations of the selected weather stations, along with climate characteristics and observation periods, are shown in Table 1. The study area includes Golmakan, Gonabad, Kashmar, Neyshabour, Mashhad, Quchan, Sarakhs, Sabzevar, Torbat-e Jam, and Torbat-e Heydarieh countries (Fig. 1). The Meteorological data used of ten synoptic meteorological stations data of Khorasan Razavi Province of Iran Meteorological Organization (IMO) are obtained from the website (https://www.irimo.ir/eng/index.php). Meteorological data included daily solar radiation (or sunshine hours), Precipitation, minimum temperature, maximum temperature, relative humidity, and wind speed. The synoptic Meteorological data have passed IMO quality control procedures such as checking situation (latitude, longitude, and elevation), tests for data homogeneity, consistency with other meteorological parameters, and data generation.

Because of the importance of accurate precipitation data for associated hydrological responses from basins and understanding climate change, in this study, the rain-gauge catch correction model proposed by (Stisen et al., 2011) is used where wind speed, rainfall intensity, and daily air temperature at grid-scale are accounted.

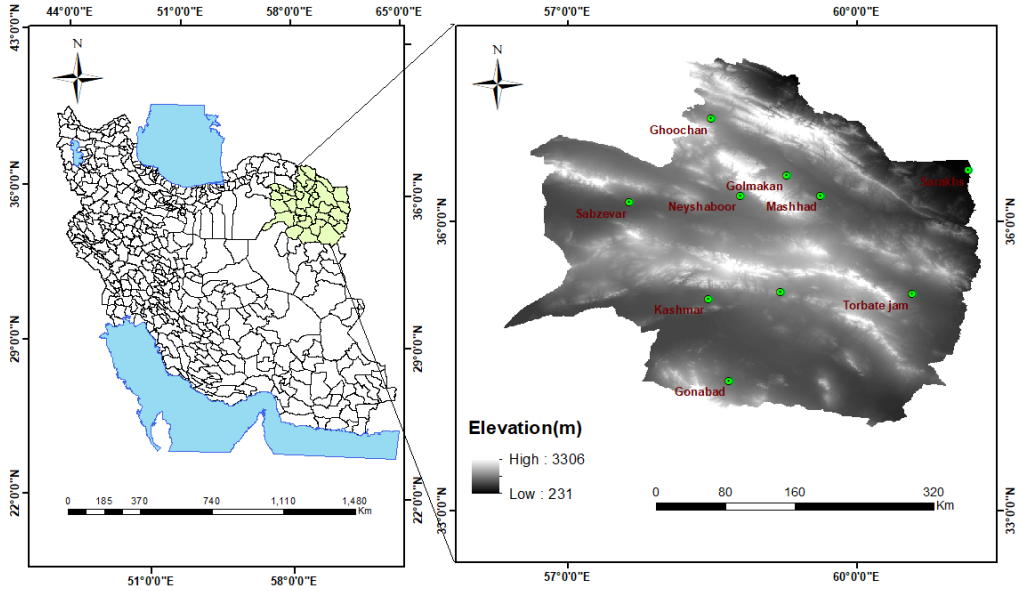


**Fig.1.** Geographical location of the study area with the spatial distribution of meteorological stations.

**Table 1.** Weather station locations and period of meteorological observations.

| Station | Longitude | Latitude | Elevation (m) | Observation period | Climate |
|---|---|---|---|---|---|
| Torbat-e Jam | 60° 35' | 35° 16' | 950.4 | 1992-2021 | Arid |
| Torbat-e Heydarieh | 59° 13' | 35° 20' | 1451.0 | 1958-2021 | Semi-arid |
| Sabzevar | 57° 39' | 36° 12' | 962.0 | 1954-2021 | Arid |
| Sarakhs | 61° 10' | 36° 32' | 235.0 | 1984-2021 | Arid |
| Quchan | 58° 30' | 37° 04' | 1287.0 | 1983-2021 | Semi-arid |
| Kashmar | 58° 28' | 35° 16' | 1110.0 | 1986-2021 | Arid |
| Golmakan | 59° 17' | 36° 29' | 1176.0 | 1986-2021 | Arid |
| Gonabad | 58° 41' | 34° 21' | 1056.0 | 1986-2021 | hyper-arid |
| Mashhad | 59° 38' | 36° 14' | 999.2 | 1950-2021 | Arid |
| Neyshabour | 58° 48' | 36° 16' | 1213.0 | 1990-2021 | Arid |

*2.2. Potential evapotranspiration (ETo) and aridity index (AI)*

A modified Penman–Monteith method (Eq. 1) was adapted to calculate the potential Evapotranspiration (ETo), which is recommended as the sole and global standard model for calculating ETo. (Fan and Thomas, 2013; Lang *et al*., 2017; Ma *et al*., 2017). The FAO Penman-Monteith (ETo) approach for estimating ETo is described as(Allen *et al*., 1998):

$$ET_o = \frac{0.408\Delta(R_n - G) + \gamma \frac{900}{T+273} u_2 (e_s - e_a)}{\Delta + \gamma(1 + 0.34u_2)} \quad (1)$$

where $ET_o$ is the daily PET rate (mm day$^{-1}$), Rn is the mean daily net radiation at the ground surface (MJ m$^{-2}$ day$^{-1}$), which was calculated from the procedure of (Allen et al., 1998), G is the soil heat flux (MJ m$^{-2}$ day$^{-1}$); T is the daily average air temperature at the height of 2 m (˚C); $u_2$ is the mean daily wind speed at a height of 2 m (m s$^{-1}$); $e_s$ and $e_a$ are the saturation vapor pressure and the actual vapor pressure

(kPa), respectively, Δ is the slope of the saturated water vapor pressure curve (kPa $^{\circ}C^{-1}$), γ is the psychrometric constant (kPa $^{\circ}C^{-1}$)

Aridity indices are a widely used criterion to describe the water-deficient of different regions. This study used four methods to assess the spatial distribution of aridity indices. The DeMartonne aridity index (in the annual, seasonal, and monthly timescale) and Pinna combinative index are based on precipitation and temperature, and Food and Agriculture Organization (FAO) aridity index, Thornthwaite aridity index is based on Precipitation and potential Evapotranspiration. The Aridity indices equations and Climate classification based on the Aridity indices in this study are shown in table 2.

**Table 2.** Climate classification based on the Aridity indices

| Aridity index | | Equation | Value of AI | Climate |
|---|---|---|---|---|
| De Martonne aridity index | The annually aridity index | $\mathrm{AI_{DMyi}} = \frac{\mathrm{P_{yi}}}{\mathrm{T_{yi}} + 10}$ | $AI_{DM}$<10 | Dry |
| | | | 10 ≤ $AI_{DM}$ < 20 | Semi-dry |
| | | | 20 ≤ $AI_{DM}$ < 24 | Mediterranean |
| | The seasonally aridity index | $\mathrm{AI_{DMsi}} = \frac{4\overline{\mathrm{P}}_{\mathrm{si}}}{\overline{\mathrm{T}}_{\mathrm{si}} + 10}$ | 24 ≤ $AI_{DM}$ < 28 | Semi-humid |
| | | | 28 ≤ $AI_{DM}$ < 35 | Humid |
| | | | 35 ≤ $AI_{DM}$ ≤ 55 | Very humid |
| | The monthly aridity index | $\mathrm{AI_{DMmi}} = \frac{12\overline{\mathrm{P}}_{\mathrm{mi}}}{\overline{\mathrm{T}}_{\mathrm{mi}} + 10}$ | $AI_{DM}$ > 55 | Extremely very humid |
| Pinna combinative index | | $AI_{\mathrm{P}i} = \frac{1}{2}\left[\frac{P_{yi}}{T_{yi}+10} + \frac{12\bar{P}_{dmi}}{\bar{T}_{\mathrm{dm}i}+10}\right]$ | $AI_p$< 10 | Dry |
| | | | 10 ≤ $AI_p$ < 20 | Semi-dry (Mediterranean) |
| | | | 20 ≤ $AI_p$ < 30 | Humid |
| | | | $AI_p$ ≥ 30 | Very humid |
| FAO aridity index | | $AI_{\mathrm{F}} = \frac{P}{ET_0}$ | $AI_F$ < 0.05 | Hyper arid |
| | | | 0.05 ≤ $AI_F$ < 0.20 | Arid |
| | | | 0.20 ≤ $AI_F$ < 0.50 | Semiarid |
| | | | 0.50 ≤ $AI_F$ < 0.65 | Dry sub-humid |
| | | | 0.65 ≤ $AI_F$ ≤ 0.75 | Wet sub-humid |
| | | | $AI_F$ > 0.75 | Humid |
| Thornthwaite aridity index | | $AI_{\mathrm{T}} = \frac{(ET_0 - P)}{ET_0}$ | If the $AI_T$ is equal to or close to 1 | it indicates that aridity is the highest |

where $AI_{DMyi}$ is value of the annually De Martonne aridity index, *Pyi* is annual precipitation in mm, and *Tyi* is annual mean temperature in °C, $AI_{DMsi}$ is value of the seasonally De Martonne aridity index, the over bar *Psi* and *Tsi* are mean seasonaly precipitation and temperature, respectively, $AI_{DMmi}$ is value of the monthly De Martonne aridity index, the over bar *Pmi* and *Tmi* are mean monthly precipitation and temperature, respectively, $AI_{pi}$ is Pinna combinative index, the over bar *Pdmi* and *Tdmi* are precipitation and temperature means in the driest month at station *i*, $AI_F$ is FAO aridity index, $AI_T$ is Thornthwaite aridity index, mean annual precipitation (*P*) and reference evapotranspiration (*ETo*).

### *2.3. The spatial distribution aridity index*

There are many interpolation methods for spatially distributing estimates of different criteria. The studies made in the spatial estimation of criteria showed that when the number of data is limited, the inverse distance-weighted (IDW) deterministic interpolation method way is a better result (Baltas, 2007; Piticar *et al*., 2016; Ma *et al*., 2017; Gebremedhin *et al*., 2018). Therefore, after the estimation of the aridity index in each station of this study area, among the various methods, the IDW method was used for the spatial assessment of the aridity index. It is an interpolation method that predicts cell importance by averaging the values of the sample data

points adjacent to each processing cell. The nearest station gets more weight than the station which is a long way from the interpolation point.

*2.4. Mann-Kendall test*

The MeK test, also called Kendall's tau test (Mann, 1945; Kendall, 1957), a nonparametric rank-based method, for assessing the significance of a trend, was widely used to analyze the changes and trends of the ETo and AI. For this purpose, the statistic S of Kendall's tau was calculated as:

$$S = \sum_{i=1}^{n-1} \sum_{j=i+1}^{2} sgn(x_j - x_i), \quad (2)$$

where n is a sample size, xi and xj are the ith and jth observations in the time series, respectively, and

$$sgn(x) = \begin{cases} +1 & if \quad (x_j - x_i) > 0 \\ 0 & if \quad (x_j - x_i) = 0 \\ -1 & if \quad (x_j - x_i) < 0 \end{cases} \quad (3)$$

(Mann, 1945) and (Kendall, 1957) have documented that the statistics S is approximately normally distributed when n ≥ 8, with the variance as follows:

$$V(S) = \frac{n(n-1)(2n+5) - \sum_{i=1}^{n} t_i(i-1)(2i+5)}{18} \quad (4)$$

Where $t_i$ is the number of ties of extent i. The standardized test statistic Zc is computed by

$$Z_c = \begin{cases} \frac{S-1}{\sqrt{var(s)}} & S > 0 \\ 0 & S = 0 \\ \frac{S+1}{\sqrt{var(s)}} & S < 0 \end{cases} \quad (5)$$

Trends were tested at two specific significance levels of α, which were 0.01, and 0.05. When |Zc| was lower than the standardized value of normal $Z_{1-\alpha/2}$, then the null hypothesis of no time series trend was accepted. Negative values of Z indicate decreasing trends, while Positive values of Z show increasing monotonic trends.

## 3. Results

The descriptive statistics of the aridity indices to demonstrate the data distributions in the study area are presented in Table 3. For the four aridity indices, the mean and median values are similar, and the skewness values were low. When the skewness coefficient is low, it indicates that the data have a normal distribution was confirmed by Kolmogorov-Smirnov tests. Distributions of the Thornthwaite aridity index were shifted to upper values because the mean values were lower than the median values. In the other three indices, the distributions of the aridity index were shifted to lowering values. However, the difference between the minimum and maximum values of the aridity index and the high values of the coefficient of variation indicates a high climatic spatial variability in the study area.

**Table 3.** Descriptive statistics of the aridity indices from 10 weather stations in study area

| Station | $AI_{DM}$ | $AI_P$ | $AI_F$ | $AI_T$ |
|---|---|---|---|---|
| Torbat-e Jam | 6.25 | 3.65 | 0.08 | 0.92 |
| Torbat-e Heydarieh | 10.38 | 9.25 | 0.19 | 0.81 |
| Sabzevar | 6.67 | 7.94 | 0.11 | 0.89 |
| Sarakhs | 6.51 | 3.44 | 0.12 | 0.88 |
| Quchan | 13.65 | 20.18 | 0.24 | 0.76 |
| Kashmar | 6.53 | 4.58 | 0.13 | 0.87 |
| Golmakan | 8.23 | 6.97 | 0.15 | 0.85 |
| Gonabad | 4.51 | 2.79 | 0.08 | 0.92 |
| Mashhad | 10.37 | 13.63 | 0.18 | 0.82 |
| Neyshabour | 9.54 | 7.04 | 0.18 | 0.82 |
| Skewness | 0.71 | 0.83 | 0.33 | -0.33 |
| Mean | 8.26 | 4.22 | 0.15 | 0.85 |
| Median | 7.45 | 3.81 | 0.14 | 0.86 |
| SD | 2.71 | 1.45 | 0.05 | 0.05 |
| MIN | 4.51 | 2.27 | 0.08 | 0.76 |
| Max | 13.65 | 7.19 | 0.24 | 0.92 |
| CV | 32.84 | 34.31 | 36.21 | 6.16 |

According to the annual values of $AI_{DM}$, seven meteorological stations in this region showed dry conditions. In comparison, three meteorological stations (Quchan, Torbat-e Heydarieh, and Mashhad) are located in the north and center of the study area classified as semi-dry conditions (Table 3). The seasonal spatial distribution of the De Martonne aridity index is shown in Figure 3. In spring, summer, and autumn seasons, all stations are classified under dry conditions, which is the driest at Gonabad station with values of 1.08 and 0.02 in spring and summer seasons respectively but in autumn season is the driest at Torbat-e Jam the value of 0.78. Regarding the winter seasonal value of $AI_{DM}$, only Quchan, Torbat-e Heydarieh, Mashhad, and Neyshabour stations showed semi-dry conditions with values of 14.80, 13.16, 11.23, and 10.91, respectively. The remaining meteorological stations are dry, which is the driest at Gonabad station with a value of 5.35. According to the monthly De Martonne aridity index, the Gonabad station in all of the months and remaining stations in all of the months except January, February, and March showed values of less than 20, which indicated that the agricultural lands need irrigation in these months (Table 4).

**Table 4.** Monthly DeMartonne aridity index value at the selected stations

| Station | Jan | Feb | Mar | Apr | May | Jun | Jul | Aug | Sep | Oct | Nov | Dec |
|---|---|---|---|---|---|---|---|---|---|---|---|---|
| Torbat-e Jam | 18.61 | 24.83 | 21.53 | 13.17 | 5.10 | 0.39 | 0.04 | 0.06 | 0.19 | 1.79 | 6.72 | 11.52 |
| Torbat-eHeydarieh | 46.47 | 43.83 | 32.22 | 18.17 | 7.65 | 1.18 | 0.20 | 0.14 | 0.30 | 2.83 | 9.16 | 29.07 |
| Sabzevar | 25.69 | 22.01 | 20.43 | 10.99 | 4.97 | 0.93 | 0.33 | 0.14 | 0.31 | 2.48 | 7.74 | 18.90 |
| Sarakhs | 20.88 | 23.74 | 22.54 | 11.48 | 3.97 | 0.27 | 0.08 | 0.01 | 0.28 | 2.74 | 8.16 | 15.13 |
| Quchan | 40.61 | 50.25 | 42.60 | 25.77 | 14.68 | 3.63 | 1.15 | 0.76 | 1.60 | 7.32 | 19.84 | 30.62 |
| Kashmar | 23.32 | 25.76 | 22.03 | 10.51 | 4.13 | 0.50 | 0.19 | 0.08 | 0.27 | 1.84 | 6.08 | 17.96 |
| Golmakan | 18.11 | 24.32 | 29.47 | 16.52 | 10.71 | 2.32 | 0.50 | 0.18 | 0.74 | 4.92 | 9.22 | 15.11 |
| Gonabad | 17.17 | 16.98 | 14.62 | 8.98 | 2.04 | 0.08 | 0.08 | 0.09 | 0.03 | 1.02 | 4.95 | 11.71 |
| Mashhad | 32.56 | 31.73 | 35.81 | 21.56 | 10.94 | 1.37 | 0.35 | 0.25 | 0.76 | 4.53 | 11.02 | 21.16 |
| Neyshabour | 30.49 | 32.25 | 34.50 | 14.78 | 8.66 | 1.82 | 0.57 | 0.16 | 0.50 | 3.25 | 13.36 | 24.04 |

*3.1. Monthly cycles of regional ETo and Thornthwaite aridity index*

Fig. 2 presents the regional monthly series for ETo, Precipitation (P), and Thornthwaite aridity index ($AI_T$) over the study area during 1950-2021. As expected, ETo exhibited strong Monthly fluctuations during the study period since it is affected by many meteorological parameters. ETo was more significant than P in all months in this area. ETo was greater than 100 mm/month during April–October and not high during December and January. In July, ETo reached a maximum with a value of 266 mm. The ETo during April– October accounted for 83% of the annual total ETo.

Fig. 2 showed that the Thornthwaite aridity index ($AI_T$) also had a significant Monthly change. In the colder November, December, and January, $AI_T$ was lower than 0.31, while $AI_T$ was higher than 0.7 from April to October. In particular, the value of $AI_T$ was higher than 0.85 and close to 1.0, from May to October, indicating an extremely arid climate in the study area which indicated means that ETo was far higher than P in these seasons. The highest $AI_T$ appeared in August, resulting in extreme drought in this region.

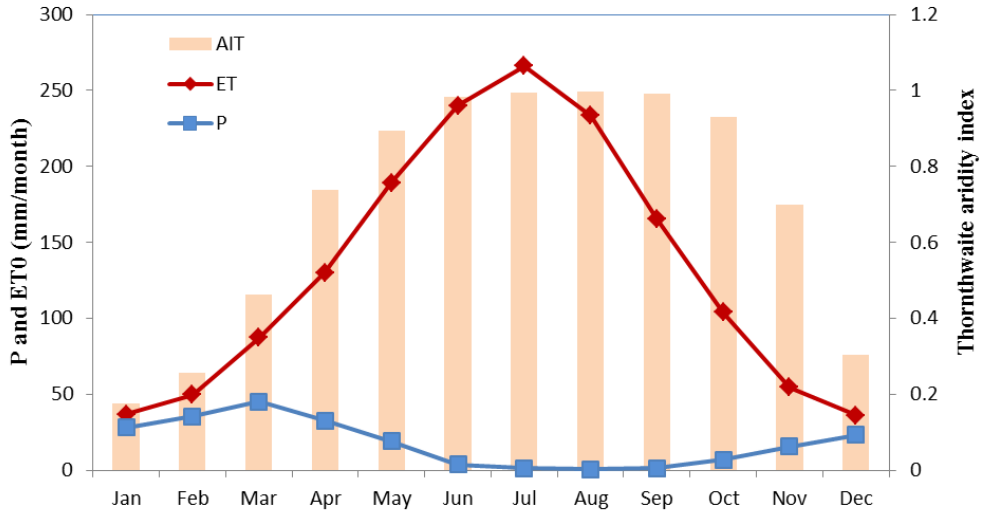


**Fig.2.** Mean monthly cycles of ETo, P, and Thornthwaite aridity index ($AI_T$) from the beginning of the statistical period of each station until 2021.

*3.2. Monthly cycles of regional Mean Temperature and the De Martonne aridity index ($AI_D$)*

$T_{mean}$ exhibited strong monthly fluctuations in this area (Fig. 3). It's monthly cycles were different from P. $T_{mean}$ was greater than P during May–October, and it was lower than P during November–April. In July, $T_{mean}$ reached a maximum with a value of 29.2 ºC. Fig. 3. showed that the DeMartonne aridity index ($AI_D$) also had a significant Monthly change. In the colder month of the year, AI was greater than 15, while $AI_D$ was lower than ten from May to November. In particular, $AI_D$ was lower than ten from May to November, indicating an arid climate, which means that $T_{mean}$ was far higher than P in these Months. The lowest $AI_D$ appeared in August, resulting in extreme drought in this region.

*3.3. Annually cycles of regional Mean Temperature and the aridity index*

Fig. 4 presents the regional annual series for Mean Temperature ($T_{mean}$), over the northern of Iran during 1951-2021. $AI_{DM}$ and $AI_p$.

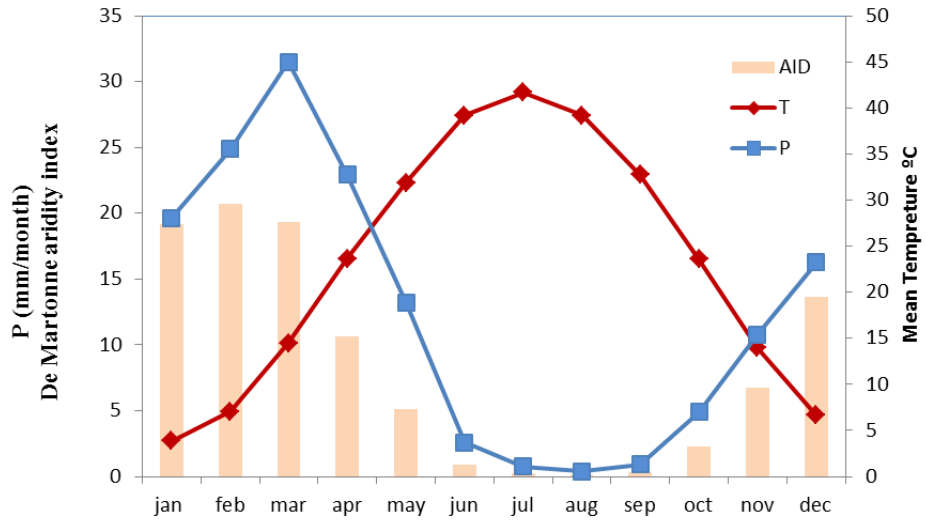


**Fig.3.** Mean monthly cycles of $T_{mean}$, P, and the De Martonne aridity index ($AI_D$) from the beginning of the statistical period of each station until 2021.

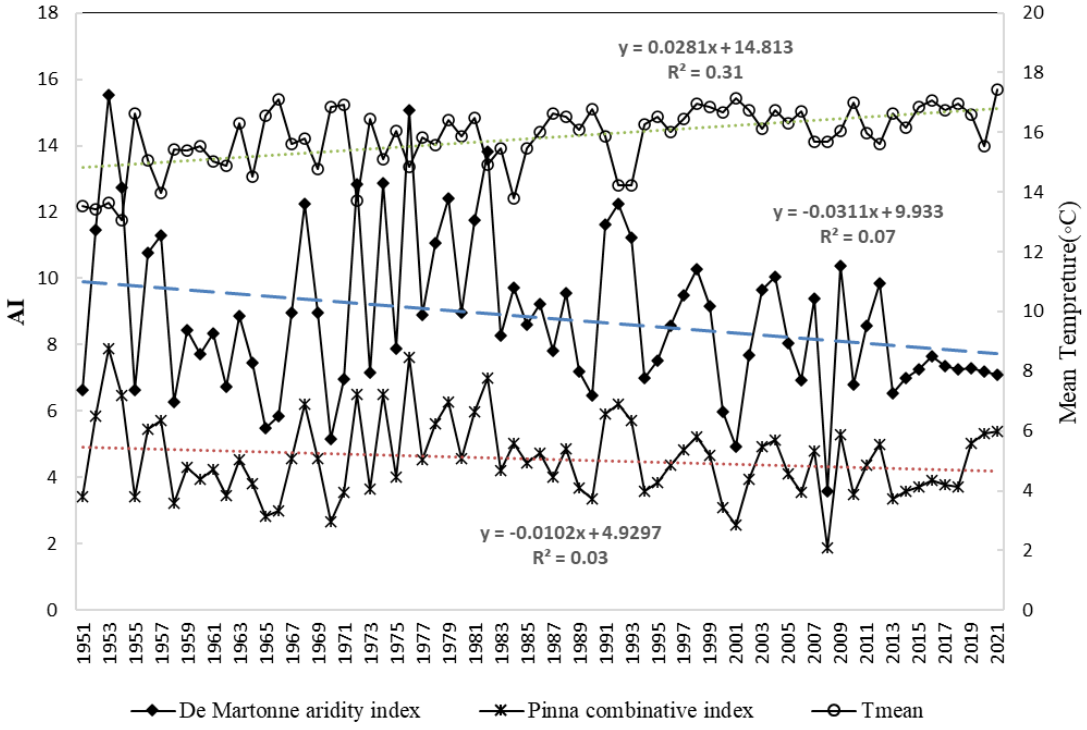


**Fig. 4.** Mean annual change of AI and $T_{mean}$ from the beginning of the statistical period of each station until 2021.

$T_{mean}$ with mean of 15.8ºC varied from 12.48-17.14 ºC during 1951-2021. $T_{mean}$ exhibited low annual fluctuations in this area (Fig. 4). The average of annual $T_{mean}$ from the beginning of the statistical period of each station until 2021 was 15.8, and for $AI_{DM}$ and $AI_p$. the average values were 8.87, and 4.58, respectively.

$T_{mean}$ exhibited significant (above 95% significance level) increasing trends in the past decades, and the regional trend was 0.03 ºC /year or 0.3 ºC/decade. Both AI ($AI_{DM}$ and $AI_p$) was not significant.

*3.4. Annually cycles of Mean regional Evapotranspiration and the aridity index*

Fig. 5 presents the regional annual series for mean evapotranspiration (ETo), $AI_T$, and $AI_F$ over the Northeastern Iran from the beginning of the statistical period of each station until 2021.

ETo with a mean of 1475.7 mm/year varied from 613.4-1867.6 ºC during 1951-2021. ETo exhibited significant annual fluctuations in this area (Fig. 5). The average annual for ETo from 1951 to 2021 was 1485.7mm. The average annual for $AI_T$, and $AI_F$ from 1951 to 2021 was for the average values were 0.84 and 0.16, respectively.

$AI_T$ and ETo have shown significant (significance level over 95%) increasing trends over the last decades. The regional trend for the two indices was 7.82mm /year or 78.2mm /decade, and 0.001 /year or 0.01/ decade, respectively. But $AI_F$ have shown significant (above 95% significance level) declining trends over the past few decades and the regional trends for this index have been -0.001/year or -0.01/decade.

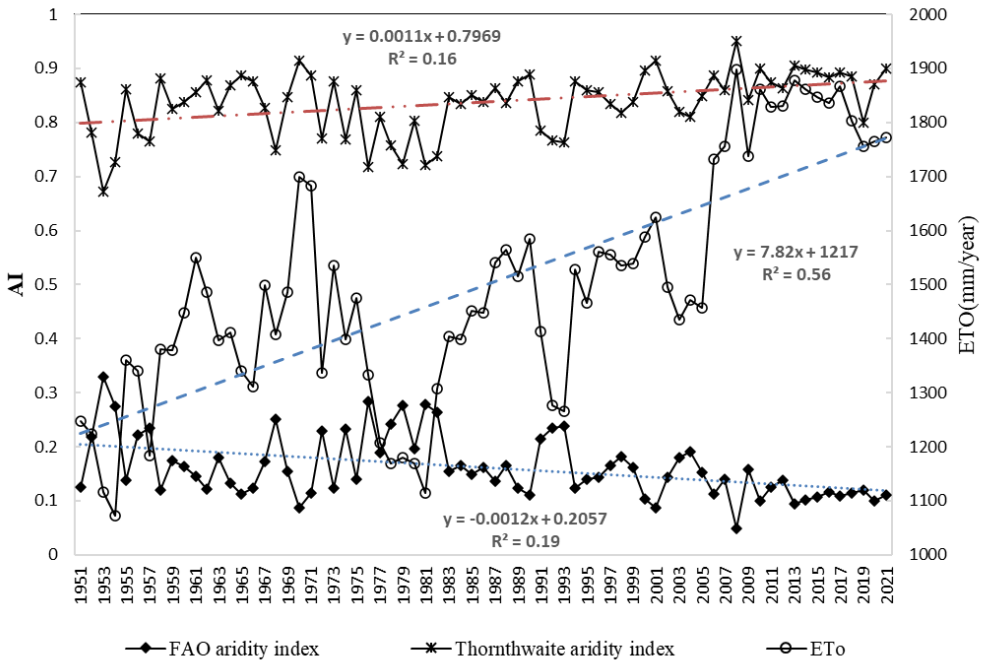


**Fig. 5.** Mean annual change of AI and ETo from the beginning of the statistical period of each station to 2021.

The low correlation coefficient observed in the study area may be attributed to temporal and spatial variations. Spatial variations, pertain to differences across geographical locations can include elevation or local weather patterns within the study area. The combination of temporal and spatial variability can lead to a weakening of the relationship between variables, resulting in a low correlation coefficient.

To further examine the properties of AI, ETo, $T_{mean}$ over the study area the

average values of AI, ETo, and $T_{mean}$ over this study area in different periods are summarized in Table 5. There were apparent increasing variations of ETo and $T_{mean}$ in different durations. The lowest and highest value of ETo and $T_{mean}$ appeared in 1951-1959 (1255.4 mm, 14.5 ºC) and 2010-2021 (1825.3 mm, 16.5 ºC), respectively. ETo and $T_{mean}$ showed an upward trend since 1950. Also, all aridity indices presented an upward trend of drought, which further demonstrated that the climate in this study area tended to be dry. The annual ETo and $T_{mean}$ annual values in these regions increased by (+)7.68 mm $year^{-1}$ per decade and (+)0.03 ºC $year^{-1}$ per decade, respectively.

These results were generally consistent with observations in northern and northwestern Iran (Tabari and Aghajanloo, 2013; Dinpashoh *et al*., 2019).

Tabari and Aghajanloo. (2013) indicated an increase in aridity was more evident in the semi-arid region of Iran. The annual ETo values in the semi-arid region increased by (+) 11.42 mm $year^{-1}$ per decade. (Nouri and Bannayan, 2019) indicated an upward trend in ETo annually for Mashhad station during 1966-2012.

**Table 5.** Average values of AI, ETo, $T_{mean}$ and P precipitation over the study area in different periods.

| Duration | $AI_T$ | $AI_F$ | $AI_P$ | $AI_{DM}$ | ETo (mm) | $T_{mean}$(ºC) | P(mm) |
|---|---|---|---|---|---|---|---|
| 1951-1959 | 0.80 | 0.20 | 5.08 | 9.97 | 1255.44 | 14.46 | 240.17 |
| 1960-1969 | 0.84 | 0.16 | 4.11 | 8.06 | 1433.66 | 15.61 | 203.90 |
| 1970-1979 | 0.81 | 0.19 | 5.10 | 10.03 | 1402.01 | 15.77 | 253.24 |
| 1980-1989 | 0.82 | 0.18 | 4.85 | 9.49 | 1391.46 | 15.72 | 237.89 |
| 1990-1999 | 0.83 | 0.17 | 4.77 | 9.36 | 1472.32 | 16.01 | 237.73 |
| 2000-2009 | 0.87 | 0.13 | 3.92 | 7.67 | 1619.52 | 16.38 | 197.46 |
| 2010-2021 | 0.88 | 0.11 | 4.22 | 7.49 | 1825.35 | 16.55 | 196.47 |

*3.5. Spatial distribution of aridity index*

The seasonal spatial distribution of $AI_{DM}$ is shown in Fig. 6. During the wintertime, almost all the study areas (73.5%) are in dry climate conditions, and the other regions (26.5%) are in Semi-dry climate conditions. During the different three seasons of the year, the whole region is in dry conditions. The spatial distribution of AIDM in the spring season is similar to the autumn season. The intensity of drought is high in summer.

The Spatial distribution of the annual ETo, $T_{mean}$, and aridity indices in the study area is shown in Fig. 7. The proportion of this region with maximum values for $T_{mean}$ was distributed in the Southwest and Northeast of this region.

The highest value of $T_{mean}$ appeared in Sarakhs located in the northeast of this region, and the lowest value was at Quchan. Meanwhile, the highest value of ETo appeared in Torbat-e Jam, situated in the Southeast of this region, and the lowest value was at Neyshabour and Quchan. Most of the areas with high ETo may reflect increased wind speed and sunshine duration (X. Zhang et al., 2009; Wang et al., 2014). The daily average of wind speed in Torbat-e Jam and Sarakhs were 4.05 and 2.3 m $s^{-1}$, respectively. Furthermore, the average sunshine duration in Torbat-e Jam and Sarakhs are 8.7 and 8 hours, respectively.

As presented in Fig. 7, generally, high ETo corresponded to the region with low $AI_F$ and high $AI_T$. According to the spatial distribution of the annual AIDM

in this region, almost all the study areas (90.6%) are in dry climate conditions, and only a tiny percentage of this area (9.6%) is in semi-arid climates that include Quchan, Mashhad, and Torbat-e Heydarieh zones. The spatial distribution of the $AID_M$ of the annual values is similar to the seasonal winter pattern.

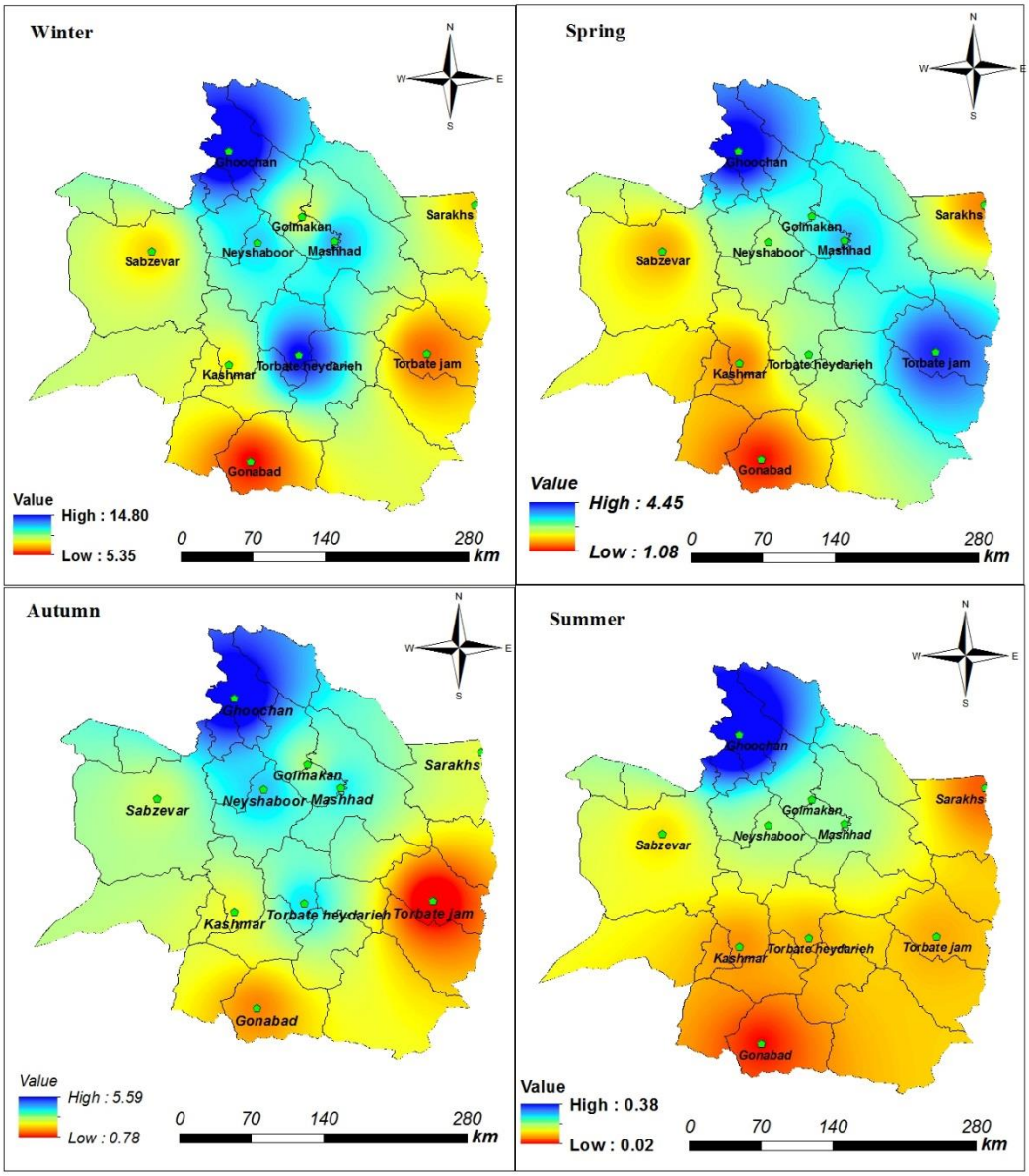


**Fig. 6.** Seasonal spatial distribution of the De Martonne aridity index in the study area.

Also, high $T_{mean}$ corresponded to the region with low $AI_{DM}$ and $AI_p$ (Fig. 7). According to the spatial $AI_P$ value, all the study areas (100%) are in dry climate conditions. The highest values of the $AI_P$ index are in the north and center of these regions include Quchan, Mashhad, and Torbat-e Heydarieh zones.

According to the spatial distribution of the annual $AI_F$ in this region, almost all the study areas (96.5%) are in dry climate conditions, and only about 3.5% of the area is in semi-arid climate including Quchan zones located in the north of this region. The spatial distributions of

$AI_F$ are similar to those obtained for the annual $AI_{DM}$ and $AI_T$. Also, the spatial distributions of $AI_P$ are identical to those obtained for the yearly $AI_F$ and $AI_{DM}$ though a more diversified distribution of climate types in this area was obtained using the $AI_F$ and $AI_{DM}$.

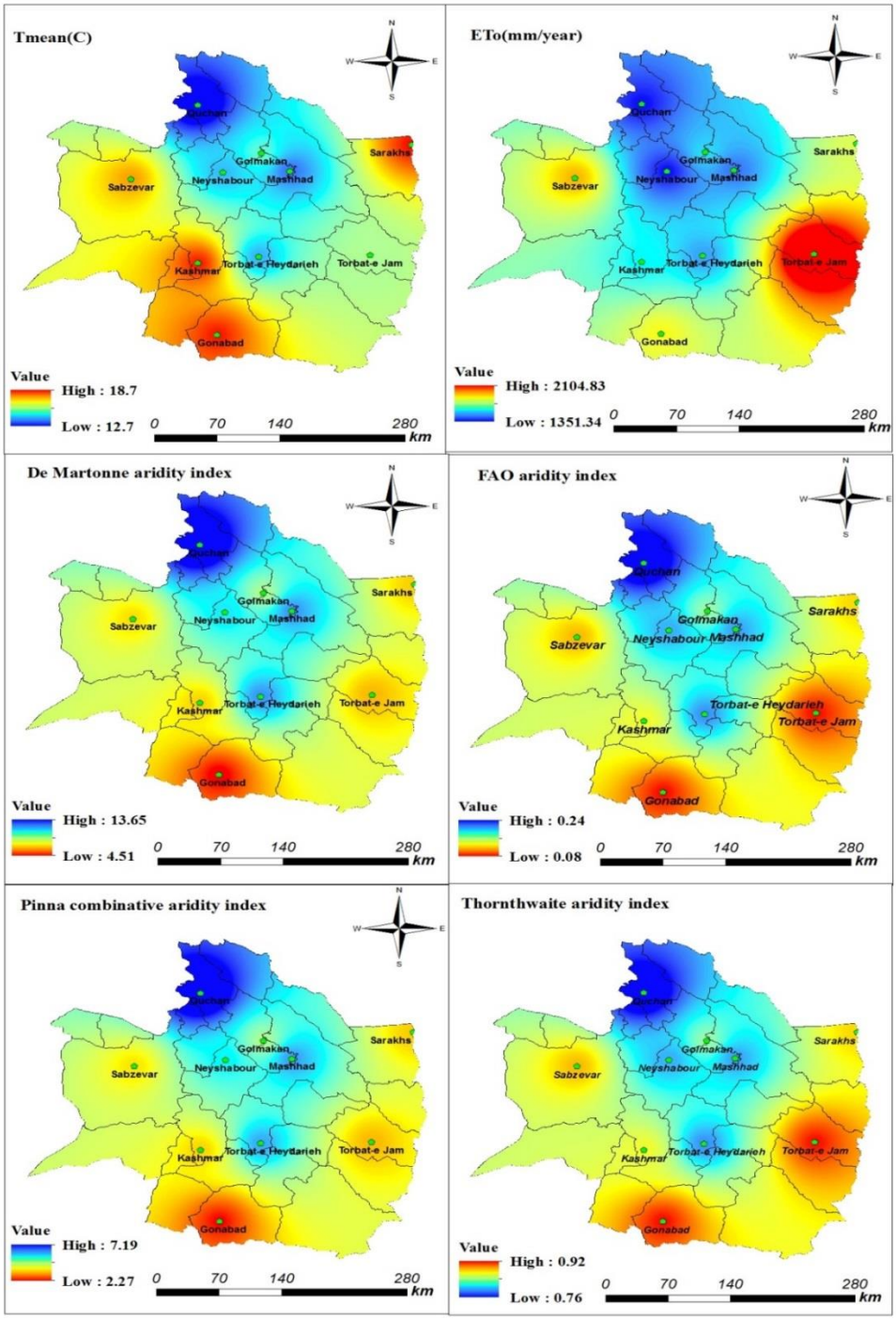


**Fig. 7.** Spatial distribution for the mean value of AI (a), $T_{mean}$, and ETo over the study area from the beginning of the statistical period of each station until 2021.

As Fig. 8 shows, all regions in the study area showed increasing trends for ETo from the beginning of the statistical period of each station until 2021, and only one station (Quchan) was

statistically significant at the 0.05 level. But the proportion of positive trends accounted for $T_{mean}$ about 50% of all stations. About 70% of the stations were statistically significant at the 0.01 level. In addition, it appeared that the north and south negative trend stations for $T_{mean}$ were the most significant in the study region. Possible explanations for the distribution pattern in the north and south are due to a decrease in wind speed up to 2.5 $ms^{-1}$ (Zhang *et al*., 2007; Shirmohammadi-Aliakbarkhani and Saberali, 2020).

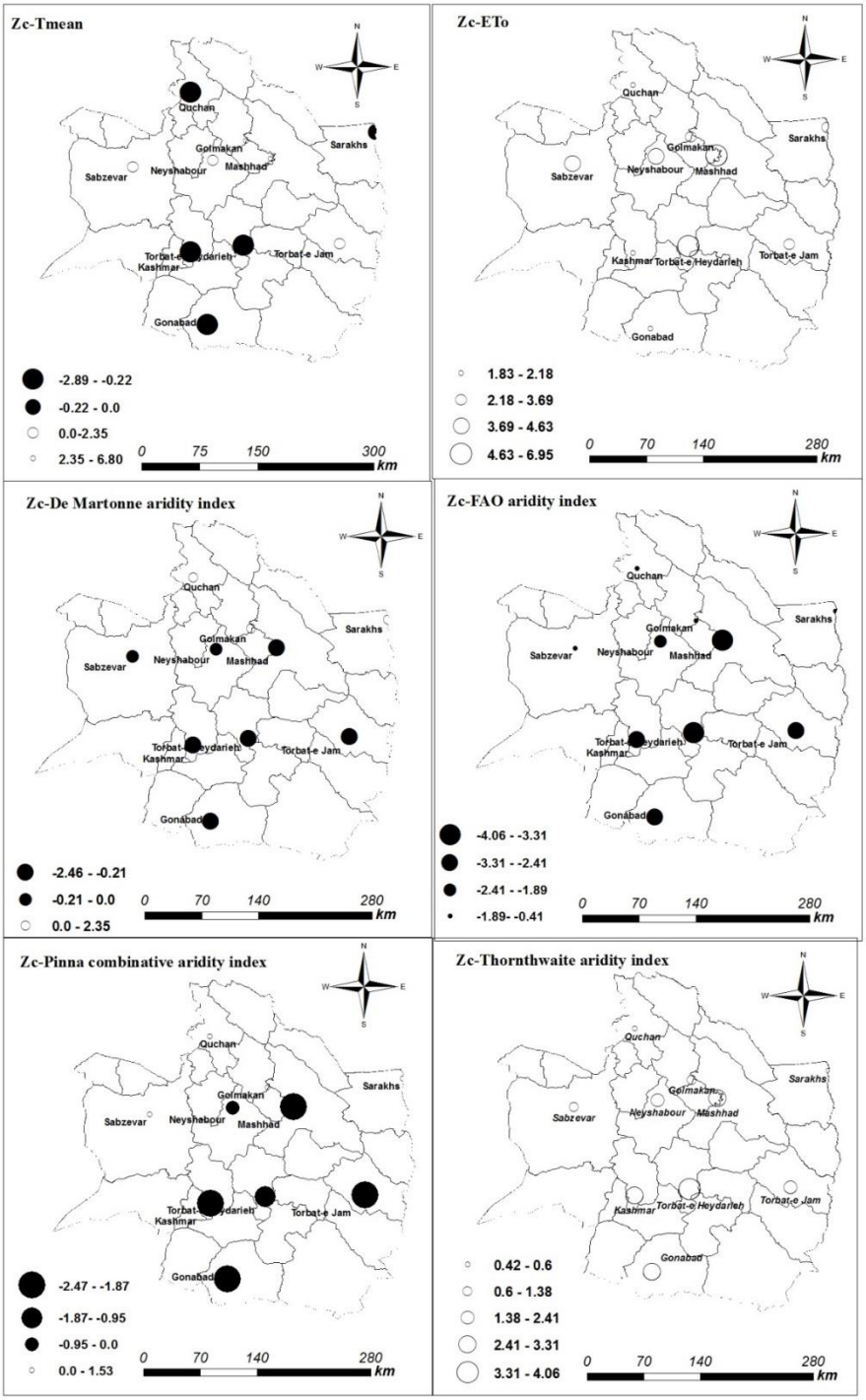


**Fig. 8.** Spatial patterns of the MK test value of $T_{mean}$, ETo, and all aridity indices in the study area from the beginning of the statistical period of each station until 2021

All of the stations generally exhibited an increasing trend for AI (positive value for $AI_T$ and negative value for $AI_{DM}$, $AI_p$, and $AI_F$), and approximately 70% of the stations showed statistically significant trends for $AI_D$ and $AI_P$ over the study area, but only 50% of the stations showed statistically significant trends for $AI_T$ and $AI_F$ over the study area (Fig. 8). Also, there were only four sites for $AI_P$ and three locations for $AI_D$ with decreasing trends that were statistically significant at the 0.01 level for $AI_P$ were mostly distributed in the north and northeastern of the study area.

## 4. Discussion

In the common imagination, aridity conjures images of drylands characterized by sparse vegetation, high temperatures, and limited surface water. While these features are indeed associated with arid regions, it's important to recognize that aridity primarily denotes a climate phenomenon characterized by water scarcity. Aridity is closely linked to water availability, typically quantified by comparing long-term precipitation or water supply to the long-term climatic water demand, known as evapotranspiration. Various models exist to describe aridity indices (AI), each varying in accuracy (Mannocchi *et al*., 2004). These indices serve critical roles in identifying climate regimes based on water availability and monitoring drought events (Moral et al., 2016). Temporal and spatial variations in AI are invaluable for understanding climate change and its impacts on ecosystem stability *(Li et al*., 2017; Cao and Zhou, 2019).

In this study, we used four aridity indices, such as the De Martonne aridity index, Pinna combinative index, FAO aridity index, and Thornthwaite aridity index. Among these indices, two indices (The De Martonne aridity index (in the annual, seasonal, and monthly timescale) and Pinna combinative indices) are based on precipitation and temperature.

The key components of AI, Precipitation, $T_{mean}$, and ETo, varied over recent years. Many studies reported that Precipitation showed a decreasing trend in Iran (Tabari and Aghajanloo, 2013; Nouri and Bannayan, 2019). In this study, the Precipitation was found to decreased from 1950 through 2021 (Table 5), particularly during 2010–2021 (−4.4 mm year−1, $p > 0.05$), but the Precipitation was more significant for 1970 - 1979 (Table 5), The abrupt decrease in Precipitation favored the intensification drought event for this region. Moreover, the ETo showed an increasing trend at 9.65 mm year−1 from 1950 to 2021. Many studies reported that the ETo showed an increasing trend in Iran (Tabari and Aghajanloo, 2013; Dinpashoh *et al*., 2019; Nouri and Bannayan, 2019). The $T_{mean}$ showed an increasing trend at the rate of 0.03 ºC year−1 from 1950 to 2021. If Precipitation decreases in Northeast Iran, the climate will be more vulnerable to severe drought.

In our research, the increasing ETo, $T_{mean}$, and decreasing precipitation led to a significant increase in all aridity indices during 1950–2021 (Table 5).

The recent decrease in precipitation and increase in temperature and evapotranspiration can be attributed to various factors including changes in climate patterns such as global warming, alterations in hydrological systems, human activities such as land-use changes and greenhouse gas emissions. These factors, individually or in combination, have impacted precipitation patterns in different regions (Ebi *et al*., 2021).

The $AI_T$, $AI_{DM}$, $AI_P$, and $AI_F$ increased significantly by +0.001, -0.03, -0.01, and -0.001, respectively. Approximately 100% of stations showed an increasing trend in $AI_T$ and $AI_F$, while 50% of stations reached a significantly increasing level, and about 60% of stations showed an increasing trend in $AI_{DM}$ and $AI_P$, while 70% of stations reached up to a considerable increasing level.

All the aridity indices show the drought situation in this region. Changes in drought indices are consistent with changes in ETo in Thornthwaite and FAo methods. However, in De

Martonne and Pinna combinative methods, although the increase in temperature in Sarakhs and Kashmar is almost similar to Gonabad, the intensity of drought in these areas is not identical to Gonabad. These variations are influenced by different local topography and regional climates. In the Kashmar station, the wind speed is comparatively lower than the Gonabad station, and the Sarakhs station was located in a relatively high latitude area combined with the Low average sunshine duration, leading to the higher values of AIDM and AIP in these areas. The positive contribution of increasing temperature to ETO was offset by the decreasing wind speed and sunshine duration in these areas. This finding is in agreement with previous results in other arid regions *(Ma et al*., 2017). Due to elevated temperatures, atmospheric water vapor deficit rises. In regions with ample surface water availability, this results in heightened actual evapotranspiration. However, in areas with limited precipitation, this exacerbates the likelihood of drought by accelerating surface drying and consequent soil moisture reduction (Stagl et al., 2014).

(Ebi *et al*., 2021) have predicted an increase in both the frequency and severity of droughts, particularly in the Mediterranean region and southern Africa.

The increasing AI would finally reduce groundwater and the stream flow in the river and impact the water availability of crops and livelihood. Investigation of the change in AI could thus improve the capability to increase management efficiency of water resources, long-term stream flow forecasting, and other guides to disaster reduction and drought resistance. Also, will improve the management of water resource.

## 5. Conclusion

The variations in the spatial and temporal characteristics of four aridity indices ($AI_{DM}$, $AI_T$, $AI_P$, and $AI_F$), $T_{mean}$, and ETo from the beginning of the statistical period of each station until 2021 were analyzed using the data from 10 meteorological stations over northeast Iran. The average annual total ETo was 1482.59 mm presenting an increasing trend of +9.65 mm/yr. Also, the annual average of $T_{mean}$ showed an increasing trend at the rate of 0.03 ºC year−1. Results indicated that all the stations had increasing ETo trends, and 10% were significant at the 5% level. But it was found that about 50% of the ten meteorological stations showed an annually increasing $T_{mean}$ trend, and 70% were significant at the 5% level. Whereas all the stations had decreasing Precipitation trends, 80% of the ten meteorological stations were significant at the 10% level. The apparent increase in the aridity index indicated that northeast Iran became drier over the last 40 years, impacting regional water resources. Such an increasing trend in ETo and $T_{mean}$ and decreasing in Precipitation trends imply that crop water requirements increased in the study area, undoubtedly. Therefore, it can be concluded that in all water-related activities, especially freshwater, the environment and agriculture, should be used scientifically. The findings of this study suggest the need to consider ETo changes in planning for water resources and agricultural projects in the dynamics of climate change, and hydrology.

## Declaration of competing interest

The authors declare that they have no conflicts of interest.

## Acknowledgments

We acknowledge the financial support received from the University of Torbat-e Jam.

## Funding

This work was supported by the Research Fund of the University of Torbat-e Jam.

## References

Allen, R. G., L. S. Pereira, D. Raes, M. Smith, 1998. Crop evapotranspiration: Guidelines for computing crop requirements. Irrigation and Drainage Paper No. 56, FAO, doi:10.1016/j.eja.2010.12.001.

Arora, V. K., 2002. The use of the aridity index to assess climate change effect on annual runoff. Journal of Hydrology,doi:10.1016/S0022-1694(02)00101-4.

Baltas, E., 2007. Spatial distribution of climatic indices in northern Greece. Meteorological Applications, doi:10.1002/met.7.

Cao, L., Z. Zhou, 2019. Variations of the reference evapotranspiration and aridity index over northeast China: Changing properties and possible causes. Advances in Meteorology,doi:10.1155/2019/7692871.

Croitoru, A. E., A. Piticar, A. M. Imbroane, D. C. Burada, 2013. Spatiotemporal distribution of aridity indices based on temperature and precipitation in the extra-Carpathian regions of Romania. Theoretical and Applied Climatology,doi:10.1007/s00704-012-0755-2.

Deniz, A., H. Toros, S. Incecik, 2011. Spatial variations of climate indices in Turkey. International Journal of Climatology,doi:10.1002/joc.2081.

Dinpashoh, Y., S. Jahanbakhsh-Asl, A. A. Rasouli, M. Foroughi, V. P. Singh, 2019. Impact of climate change on potential evapotranspiration (case study: west and NW of Iran). Theoretical and Applied Climatology,136;185–201,doi:10.1007/s00704-018-2462-0.

Djaman, K., A. B. Balde, A. Sow, B. Muller, S. Irmak, M. K. N. Diaye, B. Manneh, Y. D. Moukoumbi, K. Futakuchi, K. Saito, 2015. Journal of Hydrology : Regional Studies Evaluation of sixteen reference evapotranspiration methods under sahelian conditions in the Senegal River Valley. Journal of Hydrology: Regional Studies,3;139–159,doi:10.1016/j.ejrh.2015.02.002. Available from: http://dx.doi.org/10.1016/j.ejrh.2015.02.002.

Ebi K.L., J, Vanos, J.W. Baldwin, J.E. Bell, D.M. Hondula, N.A. Errett, K. Hayes, C.E. Reid, S. Saha, J. Spector, P. Berry, 2021. Extreme Weather and Climate Change: Population Health and Health System Implications. Annu Rev Public Health: 1;42:293-315. doi: 10.1146/annurev-publhealth-012420-105026. Epub 2021 Jan 6. PMID: 33406378; PMCID: PMC9013542.

Fan, Z. X., A. Thomas, 2013. Spatiotemporal variability of reference evapotranspiration and its contributing climatic factors in Yunnan Province, SW China, 1961-2004. Climatic Change, doi:10.1007/s10584-012-0479-4.

Gao, Y., X. Li, L. Ruby Leung, D. Chen, J. Xu, 2015. Aridity changes in the Tibetan Plateau in a warming climate. Environmental Research Letters,doi:10.1088/1748-9326/10/3/034013.

Gebremedhin, M. A., G. H. Kahsay, H. G. Fanta, 2018. Assessment of spatial distribution of aridity indices in Raya valley, northern Ethiopia. Applied Water Science,doi:10.1007/s13201-018-0868-6.

Goyal, R. K., 2004. Sensitivity of evapotranspiration to global warming: A case study of arid zone of Rajasthan (India). Agricultural Water Management,doi:10.1016/j.agwat.2004.03.014.

Herath, I. K., X. Ye, J. Wang, A. K. Bouraima, 2018. Spatial and temporal variability of reference evapotranspiration and influenced meteorological factors in the Jialing River Basin, China. Theoretical and Applied Climatology,doi:10.1007/s00704-017-2062-4.

Hosseinzadeh Talaee, P., H. Tabari, H. Abghari, 2014. Pan evaporation and reference evapotranspiration trend detection in western Iran with consideration of data persistence. Hydrology Research, doi:10.2166/nh.2013.058.

Hrnjak, I., T. Lukić, M. B. Gavrilov, S. B. Marković, M. Unkašević, I. Tošić, 2014. Aridity in Vojvodina, Serbia. Theoretical and Applied Climatology,doi:10.1007/s00704-013-0893-1.

Huntington, T. G., 2006. Evidence for intensification of the global water cycle: Review and synthesis. Journal of Hydrology,doi:10.1016/j.jhydrol.2005.07.003.

Huo, Z., X. Dai, S. Feng, S. Kang, G. Huang, 2013. Effect of climate change on reference evapotranspiration and aridity index in arid region of China. Journal of Hydrology, doi:10.1016/j.jhydrol.2013.04.011.

IPCC, 2013. Summary for policymakers [M/OL]//IPCC. Climate Change 2013: the Physical Science Basis. Cambridge University Press. Available from: http://www.climatechange2013.org/images/uploads/WGI AR5%0ASPM brochure. pdf.

Jain, S. K., R. Keshri, A. Goswami, A. Sarkar, 2010. Application of meteorological and vegetation indices for evaluation of drought impact: A case study for Rajasthan, India. Natural Hazards,doi:10.1007/s11069-009-9493-x.

Kendall, M. G., 1957. Rank Correlation Methods. 4th Edition.

Kukal, M., S. Irmak, 2016. Long-term patterns of air temperatures, daily temperature range, precipitation, grass-reference evapotranspiration and aridity index in the USA Great Plains: Part I. Spatial trends. Journal of Hydrology,doi:10.1016/j.jhydrol.2016.06.006.

Lang, D., J. Zheng, J. Shi, F. Liao, X. Ma, W. Wang, X. Chen, M. Zhang, 2017. A comparative study of potential evapotranspiration estimation by eight methods with FAO Penman–Monteith method in southwestern China. Water (Switzerland),9,doi:10.3390/w9100734.

Li, L. J., L. Zhang, H. Wang, J. Wang, J. W. Yang, D. J. Jiang, J. Y. Li, D. Y. Qin, 2007. Assessing the impact of climate variability and human activities on streamflow from the Wuding River basin in China. Hydrological Processes,doi:10.1002/hyp.6485.

Li, Y., A. Feng, W. Liu, X. Ma, G. Dong, 2017. Variation of aridity index and the role of climate variables in the Southwest China. Water (Switzerland),doi:10.3390/w9100743.

Liang, L. Q., L. J. Li, Q. Liu, 2010. Temporal variation of reference evapotranspiration during 1961-2005 in the Taoer River basin of Northeast China. Agricultural and Forest Meteorology, doi:10.1016/j.agrformet.2009.11.014.

Ma, Q., J. Zhang, C. Sun, E. Guo, F. Zhang, M. Wang, 2017. Changes of Reference Evapotranspiration and Its Relationship to Dry/Wet Conditions Based on the Aridity Index in the Songnen Grassland, Northeast China. Water,9,doi:10.3390/w9050316.

Mann, H. B., 1945. Nonparametric Tests Against Trend. Econometrica,doi:10.2307/1907187.

Mannocchi, F., F. Todisco, L. Vergni, 2004. In: Agricultural Drought: Indices Definition and Analysis the Basis of Civilization – Water Science? In: IAHS. p. 286.

de Martonne, E., 1926. Une Nouvelle fonction climatologique: L'Indice d'aridité. Impr. Gauthier-Villars. Available from: https://books.google.com/books?id=S0yycQAACAAJ.

McVicar, T. R., L. T. Li, T. G. Van Niel, L. Zhang, R. Li, Q. K. Yang, X. P. Zhang, X. M. Mu, Z. M. Wen, W. Z. Liu, Y. Zhao, Z. H. Liu, P. Gao, 2007. Developing a decision support tool for China's re-vegetation program: Simulating regional impacts of afforestation on average annual streamflow in the Loess Plateau. Forest Ecology and Management, doi:10.1016/j.foreco.2007.06.025.

Moral, F. J., F. J. Rebollo, L. L. Paniagua, A. Garc\'\ia-Mart\'\in, F. Honorio, 2016. Spatial distribution and comparison of aridity indices in Extremadura, southwestern Spain. Theoretical and applied climatology,126;801–814.

Nouri, M., M. Bannayan, 2019. Spatiotemporal changes in aridity index and reference evapotranspiration over semi-arid and humid regions of Iran: trend, cause, and sensitivity analyses. Theoretical and Applied Climatology,doi:10.1007/s00704-018-2543-0.

Paltineanu, C., I. F. Mihailescu, I. Seceleanu, C. Dragota, F. Vasenciuc, 2007. Using aridity indices to describe some climate and soil features in Eastern Europe: A Romanian case study. Theoretical and Applied Climatology,doi:10.1007/s00704-007-0295-3.

Piticar, A., D. Mihăilă, L. G. Lazurca, P. I. Bistricean, A. Puţuntică, A. E. Briciu, 2016. Spatiotemporal distribution of reference evapotranspiration in the Republic of Moldova. Theoretical and Applied Climatology,doi:10.1007/s00704-015-1490-2.

Shifteh Some'e, B., A. Ezani, H. Tabari, 2013. Spatiotemporal trends of aridity index in arid and semi-arid regions of Iran. Theoretical and Applied Climatology,doi:10.1007/s00704-012-0650-x.

Shirmohammadi-Aliakbarkhani, Z., S. F. Saberali, 2020. Evaluating of eight evapotranspiration estimation methods in arid regions of Iran. Agricultural Water Management, 239;106243, doi:https://doi.org/10.1016/j.agwat.2020.106243. Available from: http://www.sciencedirect.com/science/article/pii/S0378377420300810.

Stagl, J., E. Mayr, H. Koch, F.F. Hattermann, S. Huang, 2014. Effects of Climate Change on the Hydrological Cycle in Central and Eastern Europe. In: Rannow, S., Neubert, M. (eds) Managing Protected Areas in Central and Eastern Europe Under Climate Change. Advances in Global Change Research, vol 58. Springer, Dordrecht. https://doi.org/10.1007/978-94-007-7960-0_3

Stisen, S., T. O. Sonnenborg, A. L. Højberg, L. Troldborg, J. C. Refsgaard, 2011. Evaluation of Climate Input Biases and Water Balance Issues Using a Coupled Surface-Subsurface Model. Vadose Zone Journal,doi:10.2136/vzj2010.0001.

Tabari, H., M. B. Aghajanloo, 2013. Temporal pattern of aridity index in Iran with considering precipitation and evapotranspiration trends. International Journal of Climatology,doi:10.1002/joc.3432.

Tatli, H., M. Türkeş, 2011. Empirical Orthogonal Function analysis of the palmer drought indices. Agricultural and Forest Meteorology,doi:10.1016/j.agrformet.2011.03.004.

Thornthwaite, C. W., 1948. An Approach toward a Rational Classification of Climate. Geographical Review,doi:10.2307/210739.

Ullah, S., Q. You, D. A. Sachindra, M. Nowosad, W. Ullah, A. S. Bhatti, Z. Jin, A. Ali, 2022. Spatiotemporal changes in global aridity in terms of multiple aridity indices: An assessment based on the CRU data. Atmospheric Research, 268;105998, doi:https://doi.org/10.1016/j. atmosres. 2021. 05998. Available from: https://www.sciencedirect.com/science/article/pii/S0169809521005548.

Vasiliades, L., A. Loukas, N. Liberis, 2011. A Water Balance Derived Drought Index for Pinios River Basin, Greece. Water Resources Management,doi:10.1007/s11269-010-9665-1.

Wang, L., L. Cao, X. Deng, P. Jia, W. Zhang, X. Xu, K. Zhang, Y. Zhao, B. Yan, W. Hu, Y. Chen, 2014. Changes in aridity index and reference evapotranspiration over the central and eastern Tibetan Plateau in China during 1960-2012. Quaternary International,doi:10.1016/j.quaint.2014.07.030.

Wang, Y., T. Jiang, O. Bothe, K. Fraedrich, 2007. Changes of pan evaporation and reference evapotranspiration in the Yangtze River basin. Theoretical and Applied Climatology,doi:10.1007/s00704-006-0276-y.

Xu, X. Z., J. Y. Li, C. M. Liu, 2007. Long-term trend analysis for major climate variables in the Yellow River basin. Hydrological Processes,doi:10.1002/hyp.6405.

Zhang, Q., C. Y. Xu, M. Gemmer, D. D. Chen, C. Liu, 2009a. Changing properties of precipitation concentration in the Pearl River basin, China. Stochastic Environmental Research and Risk Assessment,doi:10.1007/s00477-008-0225-7.

Zhang, Q., C. Y. Xu, Z. Zhang, 2009b. Observed changes of drought/wetness episodes in the Pearl River basin, China, using the standardized precipitation index and aridity index. Theoretical and Applied Climatology,98;89–99,doi:10.1007/s00704-008-0095-4. Available from: https://doi.org/10.1007/s00704-008-0095-4.

Zhang, S., S. Liu, X. Mo, C. Shu, Y. Sun, C. Zhang, 2011. Assessing the impact of climate change on potential evapotranspiration in Aksu River Basin. Journal of Geographical Sciences, doi:10.1007/s11442-011-0867-0.

Zhang, X., Y. Ren, Z. Y. Yin, Z. Lin, D. Zheng, 2009. Spatial and temporal variation patterns of reference evapotranspiration across the Qinghai-Tibetan Plateau during 1971-2004. Journal of Geophysical Research Atmospheres, doi:10.1029/2009JD011753.

Zhang, Y., C. Liu, Y. Tang, Y. Yang, 2007. Trends in pan evaporation and reference and actual evapotranspiration across the Tibetan Plateau. Journal of Geophysical Research Atmospheres, doi:10.1029/2006JD008161.

Zhuguo, M., D. Li, H. Yuewen, 2004. The extreme dry/wet events in northern China during recent 100 years. Journal of Geographical Sciences,14;275–281,doi:10.1007/BF02837407. Available from: https://doi.org/10.1007/BF02837407.